Bio-based polyurethane coatings with high biomass content: tailored properties by lignin selection

Juan Carlos de Haro[a], Chiara Allegretti[a], Arjan T. Smit[b], Stefano Turri[a], Paola D'Arrigo[a,c]* and Gianmarco Griffini[a]*

paola.darrigo@polimi.it, gianmarco.griffini@polimi.it

[a] Department of Chemistry, Materials and Chemical Engineering "Giulio Natta", Politecnico di Milano, Piazza Leonardo da Vinci 32, 20133 Milano, Italy.

[b] ECN part of TNO, Biomass & Energy Efficiency, Westerduinweg 3, 1755 LE Petten, The Netherlands.

[c] Istituto di Chimica del Riconoscimento Molecolare, CNR, via Mario Bianco 9, 20131 Milano, Italy.

KEYWORDS

lignin, polyurethane, bio-based, biomass, coating, vanillic acid

ABSTRACT

New bio-based polyurethane (PU) coatings with high lignin content were developed and characterized in this work. These materials were based on a α,ω-diisocyanate monomer (1,4-bis(4-isocyanato-2-methoxyphenoxy)butane, VA-NCO) obtained from lignin-derived vanillic acid and its further crosslinking reaction with three different non-chemically-modified technical lignins obtained from different pulping processes, namely mild acetone organosolv, kraft and soda. After determining the optimal VA-NCO/lignin mass ratio for each type of lignin, an in-depth characterization of the obtained PU coatings highlighted their high biomass content, effective crosslinking, improved

1

thermal stability, hydrophobic character, good adhesion performance on different types of substrates and tunable mechanical response. These properties were found to be well correlated to the chemical-physical features of the parent lignins used (namely, molecular weight, glass transition temperature, distribution of phenylpropane subunits and -OH content), thereby suggesting the possibility to predictively tailor the characteristics of such bio-based PU coatings by lignin selection. The results of this study demonstrate that the reaction of a lignin-derived bio-based diisocyanate with different chemically unmodified technical lignins represents an interesting pathway for the production of thermosetting PU coatings with a high biomass content that can find application as high-performance bio-based materials alternative to traditional petroleum-based platforms.

Introduction

Lignin is a naturally occurring amorphous polyphenolic polymer formed from the random copolymerization of three different phenylpropane units (*p*-hydroxyphenyl, guaiacyl and syringyl) covalently linked *via* ether and C-C bonds, to form a three-dimensional network inside the cell wall of cellular plants. The proportion of these units in the molecular structure of lignin depends on its origin and extraction process, and its important effect on the properties of lignin has already been discussed in the literature.[1] Moreover, not only the structure but also the amount of lignin in lignocellulosic biomass varies depending on the original material, reaching values up to 40 wt. % in wood[2-3] whereas it usually presents values between 5 and 25 wt. % in the case of non-woody, herbaceous biomass.[4-5]

Lignin, which is produced at a rate of approximately 50 million tonnes per year,[6-7] is mainly generated as a by-product during the pulping process for cellulose isolation in the paper industry. Different de-lignification processes have been proposed and compared at industrial and laboratory scale, affecting significantly the properties of the so-obtained lignin. The kraft process is the most popular at industrial scale to isolate lignin from softwood[8] and it usually leads to the chemical degradation of lignin and to increased lignin polydispersity.[9] The soda process was proposed earlier than the kraft

process, but nowadays it is barely used at industrial scale in the paper industry and remains practically only applied to herbaceous biomass, such as sugarcane and straw.[7] In this case an increase in the content of *p*-hydroxyl units and carboxyl groups usually occurs due to thermally triggered reactions.[10] As an alternative to traditional aqueous alkali pulping processes, organosolv processes rely on the use of organic solvents to solubilise and obtain high purity lignin. A wide variety of solvents have been proposed in the literature for organosolv pulping processes including alcohols, organic acids and ketones.[11] Among these, the Fabiola[TM] organosolv process combines mild pretreatment conditions with the use of aqueous acetone as solvent. In this process, fractionation of hardwood and herbaceous biomass results in high monomeric sugar yield from the (hemi)cellulose and the isolation of a potentially less-condensed lignin.[12]

Due to its amenability to different functionalization opportunities, lignin could in principle be used as precursor for biobased materials production with tunable characteristics determined by the different pulping/delignification processes, including biorefinery concepts that are currently being developed.[13-15]

Polyurethanes (PU) are one of the most intensely produced and exploited class of polymers due to their wide field of applications as coatings, adhesives, rubbers, foams and fibers, among others.[16-17] The mechanical, thermal and chemical characteristics of PU can be tailored by selecting the proper polyol, isocyanate and catalyst, which is usually a tin derivative.[18-19] One of the most explored strategies to achieve bio-based PU involves the substitution of traditional petroleum-derived polyols by those obtained from renewable resources through different chemical approaches, including the epoxidation[20] and further ring-opening reaction of unsaturated vegetable oils[21] and the oxypropylation[22] or liquefaction[23] of lignocellulosic biomass.[22, 24] In the case of bio-polyol production through oxypropylation or liquefaction of lignocellulosic biomass, the content of lignin in the final PU product was found to barely reach 35 wt. % because the use of additional petroleum-based derivatives such as co-polyols or oxypropylation reagents is typically required.[25] A second strategy

3

to obtain bio-based PU materials consisted mainly in the chemical transformation of phenolic and aliphatic -OH moieties of industrial lignins into more reactive groups using bio-derived molecules through different functionalization processes, including esterification[26] or phenolation.[27] In these cases, the content of biomass in the final polymer could increase up to around 50 wt. %, with the polyisocyanates being the only petroleum-derived component in the PU formulation. Such biomass content can be slightly increased by using non-treated lignin as direct source of -OH groups for urethane bond formation in the absence of catalysts, as it was previously proposed in the literature.[28] As alternative to the use of biomass components as -OH source, some other authors have proposed the transformation of biomass or lignin-derived molecules into isocyanate-containing ones for the synthesis of PU through several different green or almost-green routes,[29-31] thereby avoiding the traditional pathway for the formation of isocyanates based on the use of toxic phosgene.[32] Although in some cases such bio-based isocyanates were reacted with petroleum-derived polyols to achieve PU materials,[33-34] the most interesting and sustainable route in this respect is their formulation with bio-based polyols. However, in order to reach high level of biomass content in the final material, aliphatic polyols based on vegetable oils have mainly been considered for the further production of PU,[35-37] without taking into account aromatic sources of hydroxyl moieties such as lignin. In particular, up to now no examples have appeared in the literature on the formation of PU materials by full exploitation of lignin both as source of small molecules bearing isocyanate functionalities as well as aromatic polyol macromonomer, aiming to the production of high-biomass-content thermosetting PU coatings.

To bridge this gap, novel high-biomass-content PU coatings are presented in this work based on the synthesis of a lignin-derived α-ω-diisocyanate from vanillic acid and its further polymerization with three different technical lignins obtained from three distinct delignification processes, namely organosolv, kraft and soda. The results of this study demonstrate the technical viability of obtaining high-biomass-content PU coatings with enhanced performance and tailored properties resulting from

the distinct characteristics of the type of lignin used as macromonomeric polyol in the PU formulation.

Materials and methods

Materials

4-Hydroxy-3-methoxybenzoic acid (vanillic acid, VA), sodium hydroxide (NaOH), 1,4-dibromobutane, ethyl acetate, hydrochloric acid, tetrahydrofuran (THF), triethylamine (TEA), ethyl chloroformate, sodium azide (NaN$_3$), dichloromethane, sodium sulphate, dry toluene, N-hydroxy-5-norbornene-2,3-dicarboxylic acid imide, chromium (III) acetylacetonate, dry dimethylformamide (DMF) and deuterated chloroform were purchased from Sigma Aldrich and used as received. 2-chloro-4,4,5,5-tetramethyl-1,3,2-dioxapholane was provided by Santa Cruz Biotechnology. Three different lignins were used in this work. The softwood kraft lignin (Indulin AT) was supplied by WestRock (formerly, MeadWestvaco). Due to the limited solubility of Indulin AT in the solvent used for the preparation of the PU coatings (THF), a solvent fractionation step was required in this case to isolate a THF-soluble fraction (fractionation yield of ~ 65%)[38] that was used throughout the work. The soda lignin Protobind 1000 pulped from wheat straw and Sarkanda grass was provided by Green Value and fully characterized in two previous works.[39-40] The organosolv lignin Fabiola™ was obtained from mild acetone organosolv fractionation of Rettenmayer beech as described in a recent study[12] and provided by ECN part of TNO.

Procedures

Synthesis of 4,4′-(butane-1,4-diylbis(oxy))bis(3-methoxybenzoic acid)

For the synthesis of the vanillic-based α,ω-dicarboxylic acid 4,4′-(butane-1,4-diylbis(oxy))bis(3-methoxybenzoic acid) (VA-COOH), VA and NaOH (2.5 mmol/mmol VA) were dissolved in water (5 mL/mmol VA) in a three-neck round-bottom flask equipped with a reflux condenser, a dropping funnel and a N$_2$ inlet. The mixture was kept under reflux in inert atmosphere for 1 h and then 1,4-

dibromobutane (0.5 mmol/mmol VA) was added dropwise over a period of 30 min. The reaction was left to reflux for 24 h. The mixture was then cooled and washed with ethyl acetate (1 mL/mL H_2O). The aqueous layer was acidified with HCl 6 M and the precipitate was filtered and dried under vacuum overnight, obtaining VA-COOH with a molar yield of 42%. The FTIR of parent VA and VA-COOH can be observed in Figures S1 and S2.

^{1}H NMR (d6-DMSO, 400 MHz, ppm): δ_H 1.91 (m, 4H), 3.80 (s, 6H), 4.12 (t, 4H), 7.05 (d, 2H), 7.44 (d, 2H), 7.55 (dd, 2H), 12.6 (br s, 2H); ^{31}P NMR (CDCl$_3$, 400 MHz, ppm): δ 136.18 (COOH)

Synthesis of 4,4′-(butane-1,4-diylbis(oxy))bis(3-methoxybenzoyl azide)

The synthesis of the α,ω-diacyl azide 4,4′-(butane-1,4-diylbis(oxy))bis(3-methoxybenzoyl azide) (VA-N$_3$) was performed in a three-neck round-bottom flask equipped with a reflux condenser, a dropping funnel and a N$_2$ inlet. The flask was loaded with a known amount of VA-COOH, a mixture of THF:water (3:1 v/v, 5 mL/mmol VA-COOH) and kept at 0 ºC under stirring until complete dissolution. Once the VA-COOH was completely dissolved, a solution of TEA (6 mmol/mmol VA-COOH) in THF (0.6 mL/mmol TEA) was added dropwise over 15 minutes. To the reaction mixture, ethyl chloroformate (6 mmol/mmol VA-COOH) was added over a period of 10 min and stirred for 2 h. Then, a solution of NaN$_3$ (8 mmol/mmol VA-COOH) in H$_2$O (0.2 mL/mmol NaN$_3$) was added carefully over a period of 10 min and the mixture was stirred at 0 ºC for 2 h and then at room temperature for 4 h. Ice-cold water (12.5 mL/mmol VA-COOH) was added gradually to the reaction. The formed precipitate was filtered and washed with water. The product was dissolved in dichloromethane (5 mL/mmol VA-COOH) and washed with water (7.5 mL/mmol VA-COOH), dried over anhydrous sodium sulphate, filtered and concentrated carefully under reduced pressure at 25 ºC, obtaining VA-N$_3$ as a white solid powder with a molar yield of 53%. The FTIR of VA-N$_3$ is shown in Figure S3.

^{1}H NMR (CDCl$_3$, 400 MHz, ppm): δ_H 2.09 (m, 4H), 3.89 (s, 6H), 4.19 (t, 4H), 6.88 (d, 2H), 7.5 (d, 2H), 7.65 (dd, 2H).

Synthesis of 1,4-bis(4-isocyanato-2-methoxyphenoxy)butane

The VA-based α,ω-diisocyanate 1,4-bis(4-isocyanato-2-methoxyphenoxy)butane (VA-NCO) was obtained by dissolving a VA-N$_3$ in dry toluene (5.5 mL/mmol VaN$_3$) in a three-necked round-bottom flask equipped with a reflux condenser and a N$_2$ inlet. The mixture was heated at 80 ºC for 8 h. The solvent was removed from the reaction product under reduced pressure at 60 ºC, obtaining VA-NCO as a white solid with a yield of 96%.

^{1}H NMR (CDCl$_3$, 400 MHz, ppm): δ_H 2.01 (m, 4H), 3.82 (s, 6H), 4.07 (t, 4H), 6.60 (d, 2H), 6.62 (dd, 2H), 6.78 (d, 2H).

PU synthesis and deposition process

The high-lignin content PU were prepared from the previously synthesized lignin-derived diisocyanate VA-NCO (5.21 meq NCO/g) and different amounts of lignins obtained through different pulping processes, namely organosolv (OL), kraft (KL) and soda (SL). The desired amounts of VA-NCO and lignin were dissolved at room temperature in THF at a 20 wt. % concentration under magnetic stirring. Once the mixture was completely solubilized (~ 30 min), the solution was spin-cast (1500 rpm, 40 s) onto different substrates (glass, wood, aluminum and steel) using a WS-400B-NPP spin processor (Laurell Technologies Corporation) and crosslinked in a ventilated oven during 1 h at 150 ºC, to obtain ~ 2 μm thick PU dry coatings. In order to optimize the content of VA-NCO (i.e., maximize the content of non-treated lignin) in the final PU coating, different VA-NCO/lignin mass ratios were explored for each type of lignin. The crosslinking reaction was monitored by means of Fourier-transform infrared spectroscopy, evaluating the disappearance of the N=C=O stretching signal at 2270 cm^{-1}. The determination of the FTIR spectra was made after deposition and thermal-curing of the so-prepared THF solution onto a clean and dry KBr disc.

Characterization techniques

Fourier-transform infrared spectroscopy

Fourier-transform infrared (FTIR) spectroscopy was performed on a Nicolet 760 FTIR spectrophotometer. FTIR spectra were recorded in transmission mode at room temperature in air by recording 32 accumulated scans at a resolution of 2 cm^{-1} in the 4000−400 cm^{-1} wavenumber range.

NMR spectroscopy

^{1}H NMR and ^{31}P NMR experiments were carried out on a Bruker Avance 400 spectrometer. Acquisition and data treatment were performed with Bruker TopSpin 3.2 software. ^{1}H NMR spectra were collected with a 16 ppm spectral width, 64000 points of acquisition and a relaxation delay of 1 s. As solvents, DMSO-d6 or CDCl$_3$ were selected. Chemical shifts were reported relative to internal tetramethylsilane for CDCl$_3$ and to the chemical shift of the impurities of non-deuterated solvent (i.e., δ = 2.50 ppm for DMSO-d6). In order to quantify the -OH groups in the pristine lignins, ^{31}P NMR spectra were recorded by inverse gated proton decoupling sequences using 90° pulse flip angle, with a 380 ppm spectral width, 256 scans and a relaxation delay of 5 s. Before its analyses, the lignins were dried under vacuum overnight at 40 ℃ and derivatized according to a procedure previously reported in literature.[41] As phosphitylation reagent, internal standard (IS) and relaxation reagent 2-chloro-4,4,5,5-tetramethyl-1,3,2-dioxaphospholane, N-hydroxy-5-norbornene-2,3-dicarboxylic acid imide and chromium (III) acetylacetonate were selected, respectively. The integration regions considered in this work were 152.8−152.5 ppm for the IS, 150.0−145.0 ppm for aliphatic hydroxyls, 145.0−137.0 ppm for phenolic hydroxyls, and 137.0−134.5 ppm for carboxylic hydroxyls. The obtained total OH content was further used to determine the NCO/OH molar ratio of the synthesized PU coatings.

Differential scanning calorimetry

Differential scanning calorimetry (DSC) was used to investigate the thermal transitions in the parent lignins and in the corresponding PU coatings. The measurements were performed on solid state samples (~ 10 mg) by using a Mettler Toledo DSC/823e instrument performing three runs (heating/cooling/heating) from 25 °C to 200 ℃ at a scan rate of 20 ℃/min under N$_2$ atmosphere. The

determination of the glass transition temperature (T_g) of the tested materials was based on the evaluation of the inflection point of the DSC trace in the last heating ramp.

Gel permeation chromatography

Gel permeation chromatography (GPC) was used to determine the molecular weight of parent lignins. A Waters 510 HPLC chromatograph was used equipped with a Waters 2410 refractive index detector using THF as eluent. The sample to analyse (concentration in THF 2 mg/mL, dissolution volume 200 µL) was injected into a system of columns (Ultrastyragel models HR4, HR 3 and HR 2, provided by Waters) connected in series. The chromatographic analysis was performed at 30 ºC and at a flow rate of 0.5 mL/min. Polystyrene standards in the 10^2-10^4 g/mol molecular weight range were used to calibrate the GPC system.

Thermogravimetric analysis

Thermogravimetric analyses (TGA) were performed on the parent lignins as well as on the PU coatings by means of a Q500 TGA system (TA instruments) from room temperature up to 700 ºC at a rate of 10 ºC/min. The response under both N_2 and air atmospheres was tested.

Optical contact angle

Static optical contact angle (OCA) measurements on the lignin-based PU films were performed using an OCA 20 (Data Physics) equipped with a CCD photocamera and a 500 µL Hamilton syringe at room temperature. Around 25 measurements were performed in different regions of each PU coating and the average value was recorded. Ultra-pure water and diiodomethane (DIM) were used as probe liquids.

Adhesion tests

The adhesion of the PU coatings on different substrates, namely glass (cleaned with plasma in air during 5 minutes at 150 W), wood, aluminum and stainless steel, was evaluated with a PosiTest AT-

M Manual adhesion pull-off tester (DeFelsko) by measuring the pulling force needed to detach a 20-mm diameter aluminum dolly adhered to the PU film by means of an epoxy adhesive (Araldite 2011, curing cycle: 24 h at 50 ºC).

Microindentation analysis

The mechanical properties (hardness and creep) of the PU coatings were determined by microindentation analyses. The tests were performed according to ISO 14577 using a Fischer Scope HP100 V microindenter equipped with a standard Vickers tip made of diamond. Force-controlled tests were performed, so while the test force (F) was applied the corresponding indentation depth (h) and the time were recorded.

Results and discussion

Synthesis of lignin-based isocyanate

The VA-based diisocyanate (VA-NCO) was obtained by means of a three-step-reaction process based on a previously published procedure with some slight modifications.[42] Briefly as a first step, two moles of VA reacted with 1,4-dibromobutane obtaining a VA-based α,ω-dicarboxylic acid (VA-COOH). The carboxylic groups in VA-COOH were then transformed into azides moieties with NaN_3, producing the α,ω-diacyl azide (VA-N_3). At the end the Curtius rearrangement of VA-N_3 provided the desired VA-based α,ω-diisocyanate (VA-NCO).[43] The whole reaction scheme describing the production of VA-NCO is reported in Figure 1.
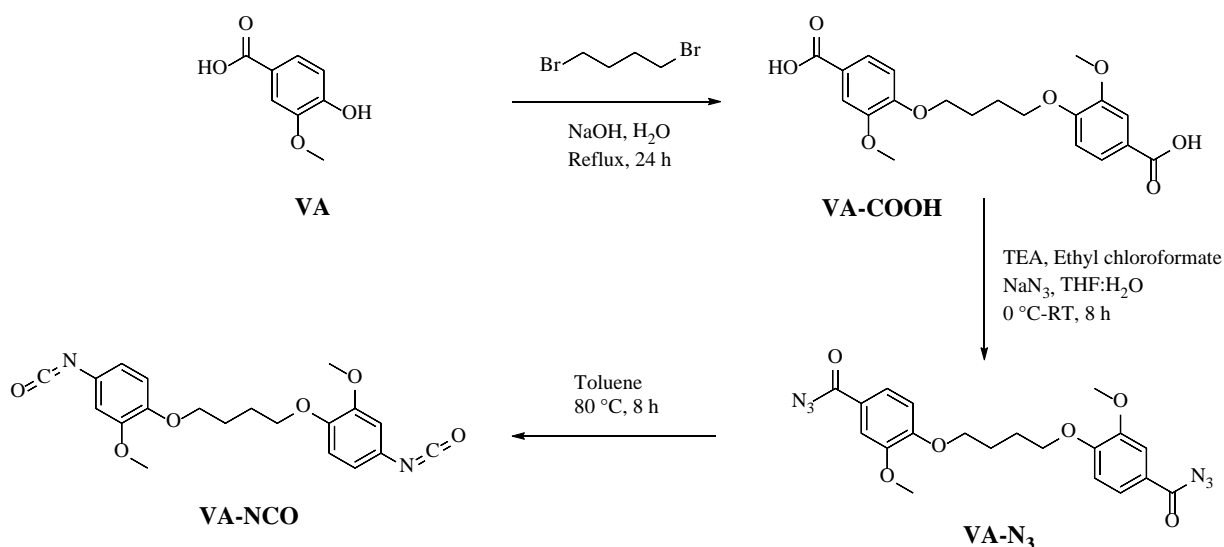
Figure 1. Reaction scheme for the production of VA-NCO from VA.

The structure of the final product (VA-NCO) was checked by means of FTIR (Figure S4). The VA-NCO presents an intense absorption band at 2270 cm^{-1} corresponding to the stretching vibration of the pendant -NCO groups. Also, two broad bands corresponding to the C-H bond stretching and aromatic structure signals were observed between 3000-2750 cm^{-1} and 1700-1500 cm^{-1}, respectively. As a proof that the pending -OCH$_3$ moieties characteristics of VA were not detached during the synthetic process, the signals corresponding to the symmetric and asymmetric vibrations of the C$_{aromatic}$-O-C$_{aliphatic}$ structure were observed at 1050 cm^{-1} and 1250 cm^{-1}. To further confirm the structure of the obtained products, ^{1}H NMR analyses were performed. Figure S5 in the Supporting Information shows the ^{1}H NMR spectra of VA-NCO where all the signals corresponding to the desired structure were observed (the ^{1}H NMR spectrum of the intermediate products VA-COOH and VA-N$_3$ are presented in Figure S6 and Figure S7 in the Supporting Information).[42]

Development of lignin-based coatings

For the preparation of the high-biomass-content PU coatings, the three types of lignin (OL, KL and SL) were crosslinked with the lignin-derived diisocyanate VA-NCO at different mass ratios. In order to determine the optimal mass ratio, the experimentation was conducted to achieve PU materials simultaneously ensuring full completion of the reaction between NCO- and OH-groups and

11

satisfactory level of crosslinking. To evaluate the extent of the NCO/OH reaction (150 ºC, 1 h), the intensity of the -NCO signal (2270 cm^{-1}) in the FTIR spectrum was monitored at different VA-NCO/lignin mass ratios and the full disappearance of that signal was taken as evidence of reaction completion. As a result, disappearance of the 2270 cm^{-1} FTIR signal was registered for maximum mass ratios of VA-NCO/OL = 0.2, VA-NCO/KL = 0.6 and VA-NCO/SL = 0.5. This indicates that for VA-NCO/lignin mass ratio equal to or lower than these values the reaction between the lignin-derived diisocyanate and hydroxyl groups in lignin has occurred to completion (lower concentrations of lignin would result in residual intensity of the -NCO stretching signal in the corresponding FTIR spectrum, as shown in Figures S8-S10 in the Supporting Information). To evaluate the level of crosslinking in the PU coatings obtained after complete NCO/OH reaction, solvent resistance (gel content) tests were performed by submerging such coatings in THF for 24 h and by evaluating the extracted sol fraction by gravimetry (Table S1). Among all the lignin-based coatings tested (VA-NCO/OL ≤ 0.2, VA-NCO/KL ≤ 0.6 and VA-NCO/SL ≤ 0.5), only those obtained at the highest VA-NCO/lignin mass ratios presented a gel content > 97%. In the other cases, a brown-coloration was found in the liquid phase, clearly indicating the presence of non-covalently-bonded lignin in the system. Hence, based on the FTIR spectra and the gel content, the maximum VA-NCO/lignin mass ratios were found to be VA-NCO/OL = 0.2, VA-NCO/KL = 0.6 and VA-NCO/SL = 0.5.

The results obtained in terms of VA-NCO/lignin mass ratios can be converted into NCO/OH molar ratios by knowing the concentration of -OH moieties present in the parent lignins. The quantification of such -OH groups was performed in this work through quantitative ^{31}P NMR analysis (Figure S11). The obtained values are reported in Table 1, expressed in mmol OH/g lignin. SL was found to possess the lowest content in -OH groups, with a total concentration of aliphatic and phenolic hydroxyl moieties of 4.04 mmol OH/g lignin. On the contrary, SL presented the highest content in -COOH groups (0.75 mmol COOH/g lignin), twice as much compared to KL (0.38 mmol COOH/g lignin) and four-times higher than in OL (0.16 mmol COOH/g). KL reported the highest total -OH content

(6.05 mmol OH/g lignin), followed by OL (5.58 mmol/g lignin). However, the proportion of aliphatic -OH groups with respect to the total -OH content was found to be higher in OL (65%) compared to KL (27%). These results are in good agreement with values previously reported in the literature for similar lignin types.[26, 44-45]

Table 1. Content in hydroxyl (aliphatic, phenolic) and carboxylic groups (expressed in mmol/g lignin), number average molecular weight (Mn) and polydispersity index (PDI) of organosolv (OL), kraft (KL) and soda lignins (SL).

Lignin	OH (aliphatic)	OH (phenolic)	COOH	Total OH	Mn (g/mol)	PDI
OL	2.20	3.38	0.16	5.58	1490	2.69
KL	1.65	4.40	0.38	6.05	970	1.70
SL	1.31	2.73	0.75	4.04	1550	5.37

From the total -OH content for the considered lignins as reported in Table 1, maximum NCO/OH molar ratios for PU coating preparations of 0.17, 0.47 and 0.58 mol/mol were determined for OL, KL and SL, respectively. These results clearly indicate that different types of lignins exhibit different reactivities of hydroxyl moieties towards –NCO. In particular, higher values of optimal NCO/OH molar ratio indicate higher lignin reactivity, i.e., a higher molar amount of VA-NCO per mole of lignin. Such differences can be rationalised based on the interplay between molecular weights and chemical-physical characteristics associated to lignins resulting from different delignification processes (i.e., either organosolv, kraft or soda).

The influence of the molecular weight of lignin on the OH-group reactivity has been previously described in the literature, where a reduction in lignin reactivity was observed when the molecular weight was increased after functionalization[46] or polymerization[47] processes. To investigate this

13

effect, GPC analyses were performed in this work and the obtained results are displayed in Table 1 (see Figure S12 in the Supporting Information for the related chromatograms). As it can be observed, SL and OL displayed similar Mn (~ 1500 g/mol), while lower values were found for KL (~ 1000 g/mol). Therefore, based on considerations purely related to the molecular weight of lignin, KL would be expected to exhibit the highest reactivity towards -NCO, while OL and SL should provide similar performance in this respect. However, the reactivity of lignin has also been shown to be affected by the type and relative abundance of monolignol repeating units in its macromolecular structure.[1, 48-49] In particular, the presence of syringyl units was shown to provide a positive effect on lignin reactivity, while high contents of guaiacyl units were found to limit it to some extent.[48] The positive effect of syringyl units on lignin reactivity could be explained based on the resonance stabilization effect provided by the electron-donating character of the two methoxy moieties during the formation of positively-charged urethane intermediate species in the polymerization process, which can compensate the expected counteracting steric hindrance effect of these two meta-substituents on the phenolic hydroxyl groups.[50-51] In order to qualitatively determine the presence and relative abundance of such repeating units in the parent lignins, FTIR analyses were performed (Figure 2) and different relative intensities (calculated considering the peak corresponding to pure aromatic skeletal vibrations at 1515 cm^{-1} as invariant band) in the characteristic absorption bands of guaiacyl (1270 cm^{-1}) and syringyl (1325 cm^{-1}) units were observed for OL, KL and SL systems. More specifically, SL and KL exhibited the highest and the lowest relative FTIR signal intensity associated to syringyl moieties, respectively. On the other hand, the guaiacyl relative signal was found to be lowest in the FTIR spectrum of OL. Therefore, following these evidences a higher reactivity of SL would be expected compared with the other lignin types. Based on these considerations and on the actual NCO/OH molar ratios experimentally found during PU coating preparation and optimization, in the case of SL the abundance of syringyl units seems to play a major role in the OH reactivity towards -NCO moieties. Conversely, the higher molecular weight seems to be the main responsible for reduced reactivity of OL compared with the other lignin types, in contrast with what observed for KL. Within this

framework, future studies will focus on beech and wheat straw organosolv lignin fractionation to obtain fractions with different molecular weight distributions for further elucidation of the relation between monolignol subunit composition, molecular weight and OH accessibility/reactivity.

In order to provide an estimate of the amount of biomass incorporated per gram of PU coating produced with the optimal NCO/OH molar ratios discussed above (from here on, PU coatings obtained from OL, KL and SL will be referred to as COL, CKL and CSL, respectively), the biomass content (BC, expressed in wt.%) in these systems was calculated considering lignin and vanillic acid as renewable carbon sources (see section S6 in the Supporting Information for details on the procedure followed and for calculations). Accordingly, values of biomass weight incorporated in the final PU coatings of 96%, 92% and 93% were found for COL, CKL and CSL, respectively. Compared with previously published results on PU coatings exploiting lignin as either isocyanate precursor or bio-based polyol[52-53], the higher biomass-content values found for the systems presented in this work further support their potential as viable bio-based PU coatings.

Characterization of PU-based coatings

FTIR analyses

To determine the chemical changes in the structure occurring during thermal curing of PU formulations to achieve the final crosslinked coatings, FTIR spectroscopy in transmission mode was used (Figure 2a). A detailed zoom of the fingerprint region (1700-1000 cm-1) is also shown (Figure 2b). All parent lignins (i.e., OL, KL and SL) present a broad absorption band between 3700 cm^{-1} and 3000 cm^{-1}, corresponding to stretching vibrations of -OH groups. This signal becomes less intense and broad in the case of lignin-derived coatings (i.e., COL, CKL and CSL), especially at 3215 cm^{-1}, because of the consumption of hydroxyl groups during the formation of urethane bonds during the reaction with VA-NCO. Further confirmation of the consumption of –OH moieties as a result of urethane-bond formation can be found by the less intense signals at 1360 and 1150 cm^{-1} corresponding to the Ph-OH groups and the C-O deformation of terminal hydroxyl groups,

respectively. The formation of the urethane linkage can be confirmed by the appearance of a shoulder related to the N-H bond (3305 cm^{-1})[54] and the signals at 1715 cm^{-1} and 1540 cm^{-1}, corresponding to C=O and C-N stretching vibrations respectively, as well as by the appearance of the N-H bending vibration signal at 960 cm^{-1}. Moreover, the presence of C-O-C bonds in hard segments (isocyanate) and in soft segments of the polymer (lignin) can be justified by the presence of two different absorption bands at 1170 cm^{-1} and 1200 cm^{-1}.[55] Additionally, a noticeable increase in the bands at 2880 cm^{-1} and 1450 cm^{-1} can be observed upon PU-coating formation, related to -CH$_2$- groups present in the C4 aliphatic chain in the lignin-derived isocyanate. Other notable signals related to the basic repeating units in lignin structure, which was previously found and discussed to play a key role in lignin reactivity, are those associated to syringyl units (absent in KL and its derived coating CKL) at 1325 cm^{-1} and guaiacyl units at 1270 cm^{-1}.[38, 56] These signals related to lignin basic structure remain practically unvaried during crosslinking, indicating the high thermal stability of the macromolecular structure of lignins during the polymerization process.
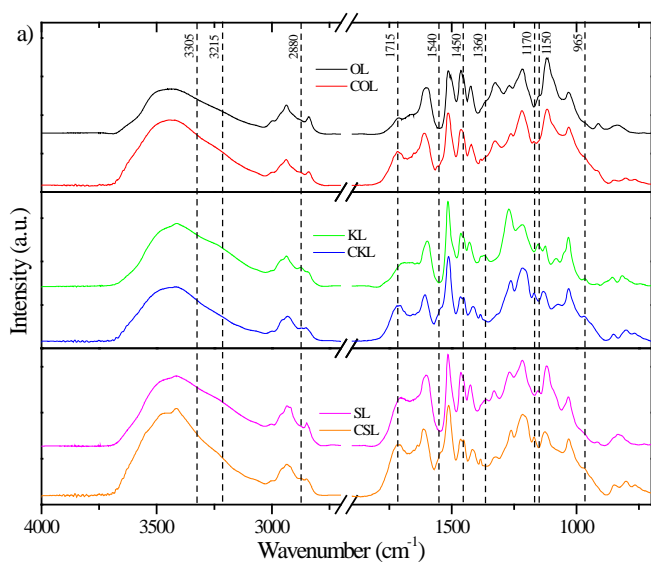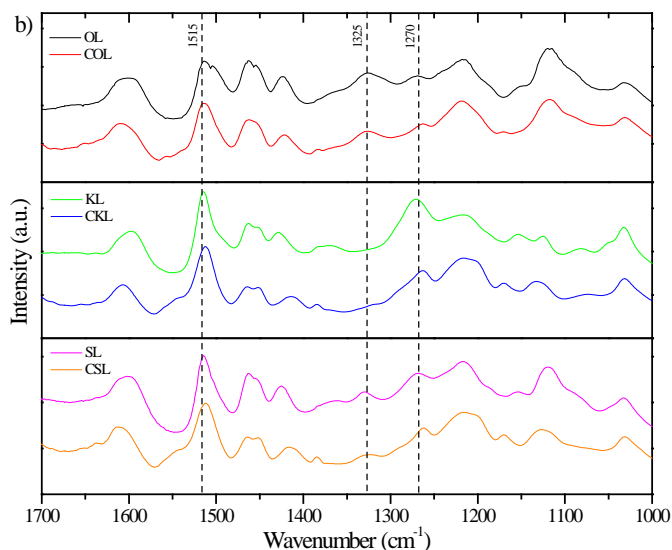
Figure 2. a) FTIR spectra of the obtained lignin-based coatings and b) fingerprint region.

Thermal characterization

The thermal transitions of the pristine lignins and the PU coatings were investigated by means of DSC and TGA. As can be observed in the DSC traces of parent lignins (Figure 3), KL is found to have the lowest T_g (105 ºC) meanwhile OL and SL reported higher T_g values (152 and 138 ºC, respectively), being all of them in good agreement with the values previously reported in literature.[38, 57] Such trends can be related to the different molecular weights of the considered lignins, as previously evidenced by means of GPC analyses (Table 1). Moreover, the higher T_g value observed for OL compared with SL may also be ascribed to the different extent of intermolecular interactions originating from H-bonded -OH groups present in the two different lignin types, being higher in the system with a higher hydroxyl group content (OL), thus yielding higher T_g.[58] The high T_g of OL, close to the crosslinking temperature (150 ºC), may affect the reactivity of this lignin towards VA-NCO to some extent. Indeed, at 150 ºC macromolecules in OL are just experimenting the transition from the glassy to the rubbery state, so their mobility is reduced thus potentially limiting their ability to react with VA-NCO. This evidence may further support the results on maximum NCO/OH molar ratios previously discussed. Upon crosslinking, an increase of T_g in all bio-based PU coatings was observed compared to the parent materials. Moreover, a single thermal transition was observed in all

17

cases, indicating that the coatings were homogeneous with no evidence of phase segregation. In particular, T_g values of 163, 135 and 146 ℃ were obtained for COL, CKL and CSL systems, respectively. The obtained T_g values are in good agreement with those previously reported in literature for analogous bio-based systems where the non-biobased TDI was used.[28] The increase in the T_g can be related to the stronger non-covalent intermolecular interactions between PU macromolecules (e.g., hydrogen bonding between unreacted -OH groups and urethane crosslinking moieties[59]) and to the increase in the molecular weight due to the crosslinking process.[60]
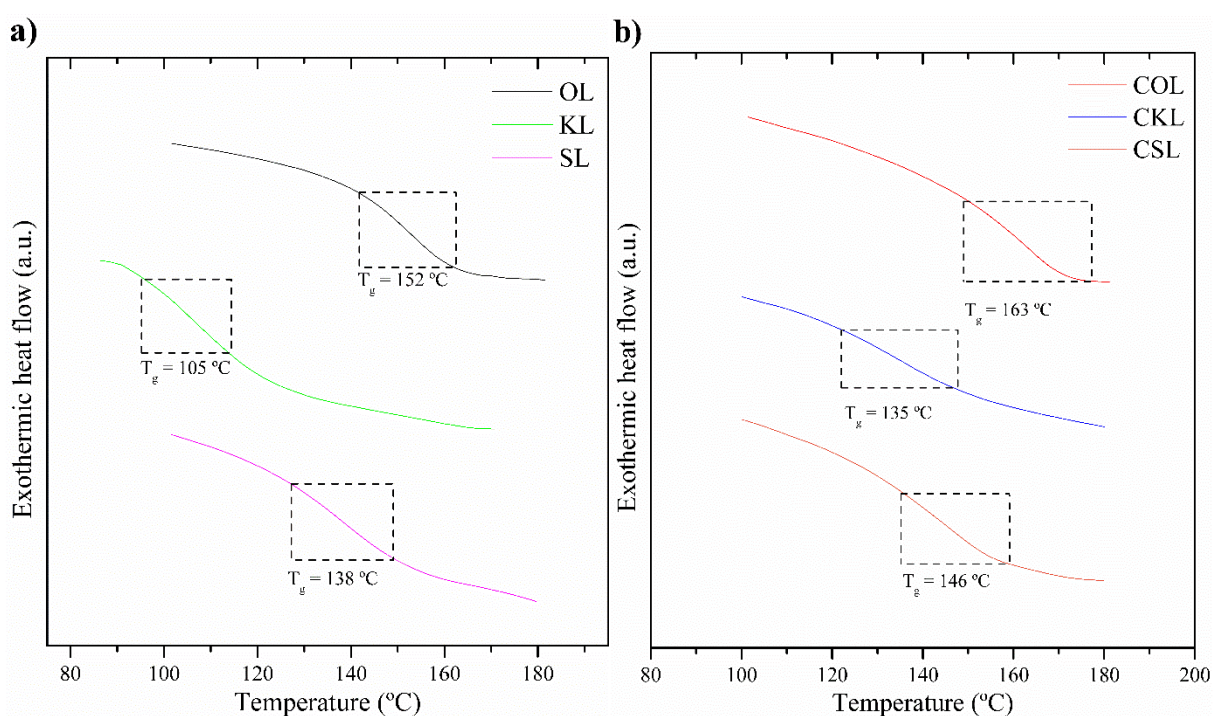

Figure 3. DSC traces of a) parent lignins and b) lignin-derived PU coatings.

TGA measurements were performed in N_2 atmosphere to analyse the thermolytic stability of the parent lignins and the PU coatings produced (Figure 4). All lignins, independently of their origin, presented a three-stage degradation profile. The first weight loss related to the evaporation of trapped solvent and water takes place at T < 150 ℃. This degradation step appears to be of higher intensity in the case of KL likely due to its higher hygroscopic character resulting from the high -OH content (see Table 1). The second degradation step takes place in the 150-300 ℃ range with a yield of 10, 13 and 17 wt. % for OL, KL and SL, respectively. The order of this weight loss correlates well with the

18

content of -COOH moieties of lignins (Table 1) and it has been previously attributed to decarboxylation reactions,[55] as well as the rupture of α- and β-alkyl-aryl ether linkages and aliphatic chains.[28] The third mass loss process occurs at T > 300 ºC and can be related to the decomposition of aromatic rings and the rupture of C-C linkages between lignin structural units and the functional groups, making it the broadest degradation step due to the variety of moieties present in lignins (phenolic hydroxyl, carbonyl and benzylic hydroxyl groups).[61] Upon crosslinking, an improvement on the thermal stability of the lignin-based PU coatings at moderate temperatures (T < 300 ºC) is observed in all cases irrespective of the parent lignin. By further increasing the temperature, a broader mass loss event was found in the coatings associated to the overlap of the previously discussed degradation of C-C bonds in the lignin structure and the degradation of the urethane moieties. Interestingly, these two degradation effects were clearly visible in CKL likely due to its higher VA-NCO content and to the lower concentration of aromatic units due to its lower molecular weight. The thermo-oxidative stability of parent lignins and lignin-based PU coatings was studied by means of TGA in air (Figure S14). As in the case of TGA analyses performed under N_2 atmosphere, also in air all the coatings presented a higher temperature of maximum degradation rate than the parent lignins. In addition, the PU coating obtained from soda lignin (CSL) exhibited the highest mass residue at 750 ºC, with a residue of around 10% of the original mass. Such noticeable improvement could be rationalised based on a two-fold effect. On the one hand, the content of elemental nitrogen in soda lignin compared with other lignins obtained from different pulping processes is higher.[10, 62] The positive impact of nitrogen in the thermal stability of different materials and its use as flame retardant has been previously discussed in the literature and its beneficial effect on PU coatings[63] and foams[64] has also been reported. On the other hand, the presence of condensed moieties on lignin structure might play an important role on the thermal stability. Soda lignins are well known to have a high concentration of condense structures generated during the biomass de-lignification process.[65-66] These condense structures might improve the thermal stability of CSL, as it was previously stated in the literature.[67]
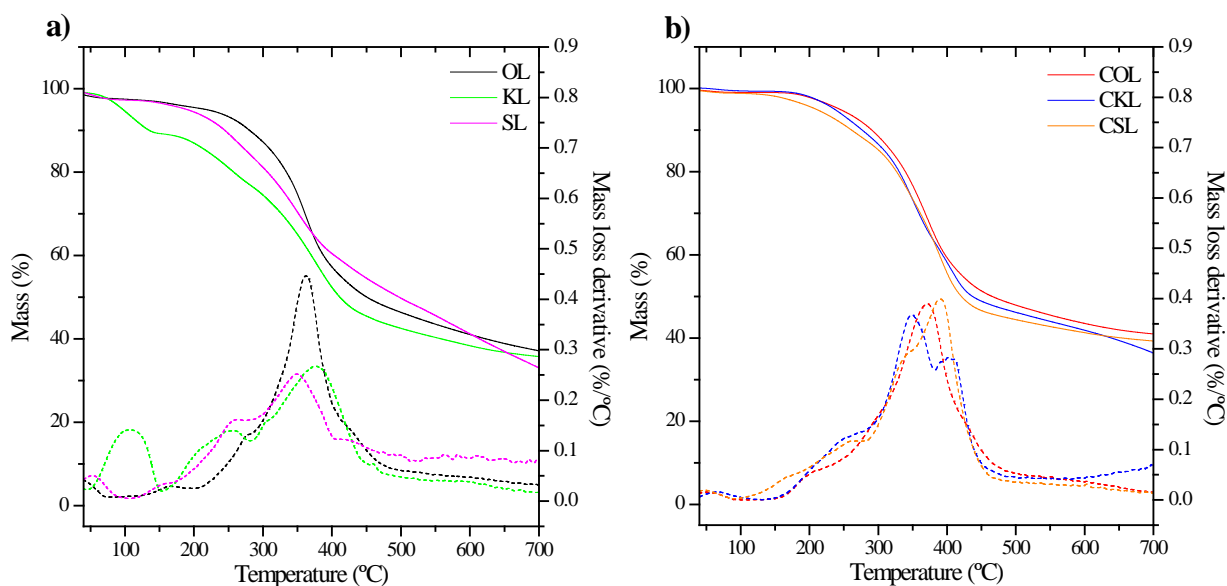
19

Figure 4. TGA analyses in N_2 atmosphere of a) parent lignins and b) PU coatings.

Optical contact angle

The wettability of the lignin-based PU coatings was investigated through the measurement of the static contact angle against water and diiodomethane (DIM) and their surface tension (γ), including its dispersive (γ^d) and polar (γ^p) components, was calculated using the Owens, Wendt, Rabel and Kaelbe (OWRK) method (Table 2).[68] Similarly to the results previously presented in literature for PU coatings from non-treated lignin and commercial petroleum-based isocyanates,[52] all PU coatings present a moderately hydrophobic character, being CSL the most hydrophobic one ($\theta_{H2O} = 104.5°$) followed by CKL ($\theta_{H2O} = 91.2°$) and COL ($\theta_{H2O} = 89.7°$). This behaviour can be attributed to the presence of residual hydroxyl groups present in lignin, as previously discussed in literature.[28] In particular, as revealed by ^{31}P NMR analyses, SL presents the lowest -OH content (Table 1) and the highest reactivity, indicating the lowest abundance of unreacted free hydroxyl moieties in CSL and hence the lowest affinity of this coating to water. On the contrary, for COL and CKL a significantly higher concentration of -OH groups (i.e., a more hydrophilic behaviour) is expected due to the higher -OH content in their parent materials and to the lower conversion of such hydroxyl groups to form

20

urethane bonds. This behaviour is also reflected in the higher value of total surface tension (γ) and its polar component (γ^p) for CSL than COL and CKL.[26]

Table 2. Static contact angles of water (θ_{H2O}) and diiodomethane (θ_{DIM}), total surface tension (γ) and its dispersive (γ^d) and polar (γ^p) components for the lignin-based PU coatings.

Coating	θ_{H2O} (º)	θ_{DIM} (º)	γ (mN/m)	γ^d (mN/m)	γ^p (mN/m)
COL	89.7 ± 3.2	48.7 ± 2.2	36.0 ± 0.5	32.2 ± 0.4	3.7 ±1.2
CKL	91.2 ± 1.4	44.6 ± 1.8	38.1 ± 0.7	34.3 ± 1.1	3.8 ± 0.9
CSL	104.5 ± 4.8	57.0 ± 6.7	30.4 ± 0.5	30.2 ± 0.4	0.2 ± 0.6

Adhesion tests

The adhesion properties of the lignin-based PU coatings were investigated by performing pull-off adhesion tests on these materials deposited onto different substrates (i.e., glass, wood, aluminum and steel). As reported in Table 3, a good adhesion with adhesive forces over 1 MPa was obtained in all the substrates irrespective of the parent lignin used, being the obtained results comparable to those previously reported in literature where a fraction of kraft lignin and the petroleum-derived toluene diisocyanate (TDI) were used.[28] The highest adhesive strength was found on glass, obtaining results over the maximum allowable reading of the instrument (9 MPa) and indicating very good bonding performance. This result may be explained by considering the non-covalent interactions of hydroxyl moieties of lignin with the oxygen groups in glass, which are favoured thanks to the plasma pre-treatment.[69] Similarly, the noticeable good adhesion on wood can be explained by considering the lignocellulosic nature of lignins and its high chemical affinity with wood as well as the presence of natural pores in wood that allow a physical grafting of the coated material.[70] In this respect, it has to be noted that the reported values for the adhesion force on wood are underestimated since the detachment of the dolly from the wood substrates was only partial. In addition, the adhesion forces were found to be slightly higher on steel than on aluminium, likely due to the stronger hydrogen

bonding interactions between the former and the coatings which are partially inhibited by the presence of a naturally formed Al_2O_3 passivation layer on the latter. Interestingly, the adhesion strengths observed in these systems compare well with some other lignin-based PU[28, 71] and polyester[26] coatings recently reported in literature, suggesting the viability of these high lignin content materials as primers in multi-layered coatings.

Table 3. Adhesive strength of the PU lignin-based coatings on different substrates.

Coating	Adhesion force (MPa)			
	Glass	Wood	Aluminum	Steel
COL	>9[a]	1.21 ± 0.21[b]	1.02 ± 0.11	1.28 ± 0.14
CKL	>9	1.28 ± 0.36[b]	1.06 ± 0.04	1.28 ± 0.19
CSL	>9	1.63 ± 0.07[b]	1.17 ± 0.28	1.40 ± 0.24

[a]9 MPa represents the maximum allowable instrumental reading
[b]Partial detachment of the lignin-based PU coating

Microindentation tests

Microindentation tests were performed on the PU coatings to study the surface hardness and the viscoelastic behaviour of the materials based on the Vickers indentation hardness (H_{IT}), indentation modulus (E_{IT}), indentation creep ($C_{IT,1}$) and creep recovery after the load release ($C_{IT,2}$). According to the standard procedure followed during the microindentation tests (ISO 14577), E_{IT} can be considered comparable with the Young's modulus of the coatings in the absence of pile-up and sink-in, not present in this case. A detailed description of the measurement protocol adopted and a definition of the parameters investigated is included in the Supporting Information (Figure S15). Representative microindentation traces for all lignin-based coating systems analysed in this work (COL, CKL and CSL) are shown in Figure 5 and the obtained results are summarized in Table 4.
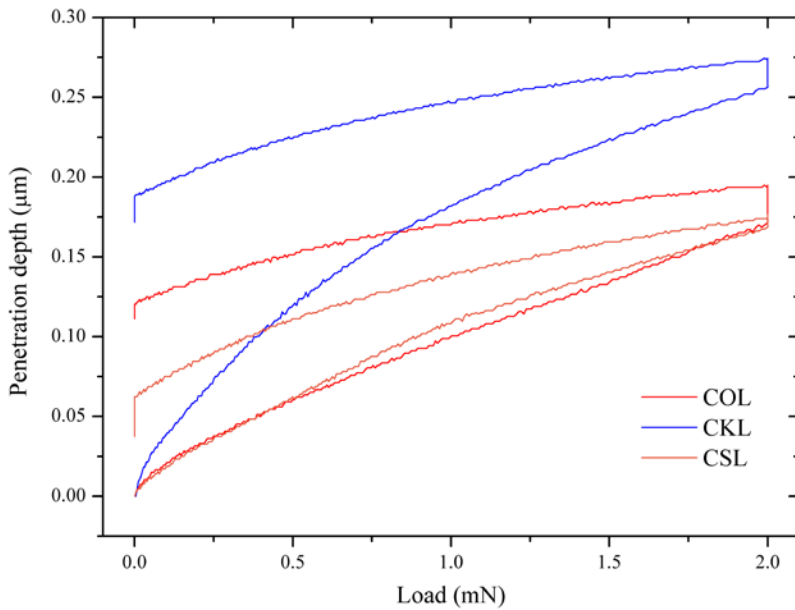
Figure 5. Representative indentation traces obtained from tests on the PU coatings COL, CKL and CSL.

COL presented the highest H_{IT} value (853 N/mm^2), in agreement with the higher T_g observed for this coating (163 ºC). CKL and CSL exhibited slightly lower H_{IT} values, around 840 N/mm^2, according to their more moderate T_g values (135 and 146 ºC, respectively). Similarly, COL was found to possess the highest indentation modulus, with an E_{IT} of 17.3 GPa, followed by CKL and CSL with values of 12.5 and 12.1 GPa, respectively. This close relation between T_g and the hardness of the material was previously discussed in literature.[72-73] Moreover, since the materials presented a high E_{IT} and a moderately high T_g, the obtained lignin-based PU coatings can be considered relatively rigid and stiff. It has to be noted that, the high E_{IT} values reported for all the coatings might indicate some contribution provided by the glass substrate, in spite of the maximum indentation depth was approximately the 10% of the coating thickness.[73]

In terms of indentation creep and recovery, CSL was found to exhibit the lowest creep during the indentation process ($C_{IT,1} = 4.7\%$) and the highest recovery after load release ($C_{IT,2} = 7.2\%$), indicating its higher elasticity. On the other hand, COL presented the highest indentation creep and the lowest creep recovery, with values of 6.9% and 3.7%, respectively; an intermediate behavior was instead observed for CKL. These results appear to be in good agreement with the VA-NCO/lignin weight

ratios (e.g., lignin mass fractions) employed in the analysed coatings, whose maximum values were found to be directly influenced by the chemical-physical characteristics of the selected lignin (relative abundance of the repeating units, molecular weight): COL exhibited the highest lignin mass fraction, followed by CKL and CSL. Since creep deformation is directly correlated with the viscoelastic nature of polymeric materials, these trends may be explained by considering that coatings with a larger mass amount of polymeric component (lignin) will tend to exhibit larger deformation due to creep and lower creep recovery, as observed in the case of COL. This can also be associated to a lower density of crosslinking, as a result of the high T_g of this material.

Table 4. Microindentation results obtained on the high-lignin-content PU coatings. T_g values and VA-NCO/lignin ratio are also reported for easy reference.

Coating	H_{IT} (N/mm^2)	E_{IT} (GPa)	$C_{IT,1}$ (%)	$C_{IT,2}$ (%)	T_g (ºC)	VA-NCO/lignin mass ratio
COL	853 ± 8	17.3 ± 0.9	6.9 ± 0.9	$(-)3.7 \pm 0.7$	163	0.2
CKL	835 ± 6	12.5 ± 0.6	6.7 ± 0.4	$(-)7.2 \pm 0.1$	135	0.6
CSL	847 ± 3	12.1 ± 0.4	4.7 ± 0.7	$(-)7.2 \pm 0.6$	146	0.5

Conclusions

New high-lignin-content PU coatings were developed and characterized in this work. These materials were obtained by synthesizing a vanillic-acid-derived α,ω-diisocyanate (VA-NCO) and its further reaction with three different chemically unmodified technical lignins produced through various pulping processes, namely organosolv (OL), kraft (KL) and soda (SL). The maximum achievable VA-NCO/lignin mass ratios were determined based on chemical analysis through FTIR spectroscopy and gel-content measurements, and the corresponding maximum NCO/OH molar ratios were calculated by quantification of the hydroxyl content in the three different lignins by means of [31]P

NMR analysis. Based on these considerations, a maximum biomass content in the obtained PU coatings in the 92-96 wt. % range was estimated, which is among the highest values reported so far in the literature for lignin-based PU materials. DSC analyses showed an increase in the T_g of all PU coatings compared to the corresponding parent lignins, thus indicating the occurrence of the crosslinking reaction. In addition, a single thermal transition for each lignin-based coating ranging from 135 to 163 ºC was observed, indicating the monophasic nature of the obtained coatings and the strong effect on T_g of the parent lignin system employed as macropolyol for their formation. The improved thermal stability was further confirmed by means of TGA analyses in N_2 and air atmosphere. Contact angle measurements revealed a moderately hydrophobic character for all PU coatings. The adhesion on different substrates was determined by means of pull-off tests, yielding good adhesion values on wood, aluminum, steel and glass. Finally, the high-lignin-content PU coatings were assessed in terms of their mechanical behaviour, and clear correlations between their hardness and their T_g were observed in addition to a direct dependence of the viscoelastic behavior of the coating materials on their lignin mass fraction.

The results of this study show for the first time that the formulation of bio-based PU coatings starting from chemically unmodified technical lignins as macropolyols and a lignin-derived diisocyanate based on vanillic acid is a promising strategy for the development of thermosetting systems with very high biomass content.

The PU coatings presented here exhibit chemical-physical properties that can be easily tuned based on the lignin precursor employed for their preparation, thus opening the way towards the production of bio-based PU coatings with tailored characteristics.

Acknowledgements

with improved economic and environmental performance"). Gigliola Clerici is greatly acknowledged for her kind support in the thermal analysis measurements.

Supporting information. The file is available free of charge and contains: FTIR spectra of VA-NCO; ^{1}H NMR spectra of VA-NCO and intermediate products; FTIR spectra at different VA-NCO/lignin ratios; procedure for gel content determination; ^{31}P NMR spectra and GPC traces of parent lignins; details on the determination of the biomass content and microindentation tests; TGA traces.

Corresponding Author

*gianmarco.griffini@polimi.it

*paola.darrigo@polimi.it

Author Contributions

The manuscript was written through contributions of all authors. All authors have given approval to the final version of the manuscript.

References

1.   Sun, Y.; Qiu, X.; Liu, Y., Chemical reactivity of alkali lignin modified with laccase. *Biomass Bioenergy* **2013,** *55*, 198-204, DOI 10.1016/j.biombioe.2013.02.006.

2.   Kline, L. M.; Hayes, D. G.; Womac, A. R.; Labbé, N., Simplified determination of lignin content in hard and soft woods via UV-spectrophotometric analysis of biomass dissolved in ionic liquids. *BioResour.* **2010,** *5* (3), 1366-1383, DOI 10.15376/biores.5.3.1366-1383.

3.   Fu, L.; McCallum, S. A.; Miao, J.; Hart, C.; Tudryn, G. J.; Zhang, F.; Linhardt, R. J., Rapid and accurate determination of the lignin content of lignocellulosic biomass by solid-state NMR. *Fuel* **2015,** *141*, 39-45, DOI 10.1016/j.fuel.2014.10.039.

4.   Lupoi, J. S.; Smith, E. A., Characterization of woody and herbaceous biomasses lignin composition with 1064 nm dispersive multichannel Raman spectroscopy. *Appl Spectrosc* **2012,** *66* (8), 903-910, DOI 10.1366/12-06621.

5.   Maucieri, C.; Camarotto, C.; Florio, G.; Albergo, R.; Ambrico, A.; Trupo, M.; Borin, M., Bioethanol and biomethane potential production of thirteen pluri-annual herbaceous species. *Ind. Crops Prod.* **2019,** *129*, 694-701, DOI 10.1016/j.indcrop.2018.12.007.

6.   Agarwal, A.; Rana, M.; Park, J. H., Advancement in technologies for the depolymerization of lignin. *Fuel Process. Technol.* **2018,** *181*, 115-132, DOI 10.1016/j.fuproc.2018.09.017.

7.   Tribot, A.; Amer, G.; Abdou Alio, M.; de Baynast, H.; Delattre, C.; Pons, A.; Mathias, J. D.; Callois, J. M.; Vial, C.; Michaud, P.; Dussap, C. G., Wood-lignin: Supply, extraction processes and use as bio-based material. *Eur. Polym. J.* **2019,** *112*, 228-240, DOI 10.1016/j.eurpolymj.2019.01.007.

8.   Gellerstedt, G., Softwood kraft lignin: Raw material for the future. *Ind. Crops Prod.* **2015,** *77*, 845-854, DOI 10.1016/j.indcrop.2015.09.040.

9.   Froass, P. M.; Ragauskas, A. J.; Jiang, J. E., NMR Studies Part 3: Analysis of Lignins from Modern Kraft Pulping Technologies. *Holzforschung* **1998,** *52* (4), 385-390, DOI 10.1515/hfsg.1998.52.4.385.

10.   Vishtal, A.; Kraslawski, A., Challenges in industrial applications of technical lignins. *BioResour.* **2011,** *6* (3), 3547-3568, DOI 10.15376/biores.6.3.3547-3568.

11.   Brosse, N., Organosolv lignins: Extraction, characterization and utilization for the conception of environmentally friendly materials. In *Lignin: Properties and Applications in Biotechnology and Bioenergy*, Nova Science Publishers, Inc.: 2012; pp 381-402.

12.   Smit, A.; Huijgen, W., Effective fractionation of lignocellulose in herbaceous biomass and hardwood using a mild acetone organosolv process. *Green Chem.* **2017,** *19* (22), 5505-5514, DOI 10.1039/c7gc02379k.

13.   Chung, H.; Washburn, N. R., Extraction and Types of Lignin. In *Lignin in Polymer Composites*, Elsevier Inc.: 2015; pp 13-25.

14.   Lancefield, C. S.; Constant, S.; Peinder, P. d.; Bruijnincx, P. C. A., Linkage Abundance and Molecular Weight Characteristics of Technical Lignins by Attenuated Total Reflection-FTIR Spectroscopy Combined with Multivariate Analysis. *ChemSusChem* **2019**, DOI 10.1002/cssc.201802809.

15.   Laurichesse, S.; Avérous, L., Chemical modification of lignins: Towards biobased polymers. *Prog. Polym. Sci.* **2014,** *39* (7), 1266-1290, DOI 10.1016/j.progpolymsci.2013.11.004.

16.   Engels, H.-W.; Pirkl, H.-G.; Albers, R.; Albach, R. W.; Krause, J.; Hoffmann, A.; Casselmann, H.; Dormish, J., Polyurethanes: Versatile Materials and Sustainable Problem Solvers for Today's Challenges. *Angew. Chem. Int. Ed.* **2013,** *52* (36), 9422-9441, DOI doi:10.1002/anie.201302766.

17.   D'Arrigo, P.; Giordano, C.; Macchi, P.; Malpezzi, L.; Pedrocchi-Fantoni, G.; Servi, S., Synthesis, platelet adhesion and cytotoxicity studies of new glycerophosphoryl-containing polyurethanes. *Int. J. Artif. Organs* **2007,** *30* (2), 133-143, DOI 10.1177/039139880703000208.

18.   Narayan, R.; Chattopadhyay, D. K.; Sreedhar, B.; Raju, K. V. S. N.; Mallikarjuna, N. N.; Aminabhavi, T. M., Synthesis and characterization of crosslinked polyurethane dispersions based on hydroxylated polyesters. *J. Appl. Polym. Sci.* **2006,** *99* (1), 368-380, DOI 10.1002/app.22430.

19.   Acetti, D.; D'Arrigo, P.; Giordano, C.; Macchi, P.; Servi, S.; Tessaro, D., New aliphatic glycerophosphoryl-containing polyurethanes: Synthesis, platelet adhesion and elution cytotoxicity studies. *Int. J. Artif. Organs* **2009,** *32* (4), 204-212, DOI 10.1177/039139880903200404.

20.   de Haro, J. C.; Izarra, I.; Rodríguez, J. F.; Pérez, Á.; Carmona, M., Modelling the epoxidation reaction of grape seed oil by peracetic acid. *J. Clean. Prod.* **2016,** *138*, 70-76, DOI 10.1016/j.jclepro.2016.05.015.

21.   de Haro, J. C.; López-Pedrajas, D.; Pérez, Á.; Rodríguez, J. F.; Carmona, M., Synthesis of rigid polyurethane foams from phosphorylated biopolyols. *Environ. Sci. Pollut. Res.* **2017**, 1-10, DOI 10.1007/s11356-017-9765-z.

22.   Evtiouguina, M.; Barros-Timmons, A.; Cruz-Pinto, J. J.; Neto, C. P.; Belgacem, M. N.; Gandini, A., Oxypropylation of Cork and the Use of the Ensuing Polyols in Polyurethane Formulations. *Biomacromolecules* **2002,** *3* (1), 57-62, DOI 10.1021/bm010100c.

23.   Hu, S.; Wan, C.; Li, Y., Production and characterization of biopolyols and polyurethane foams from crude glycerol based liquefaction of soybean straw. *Bioresour. Technol.* **2012,** *103* (1), 227-233, DOI 10.1016/j.biortech.2011.09.125.

24.   Pavier, C.; Gandini, A., Urethanes and polyurethanes from oxypropylated sugar beet pulp: I. Kinetic study in solution. *Eur. Polym. J.* **2000,** *36* (8), 1653-1658, DOI https://doi.org/10.1016/S0014-3057(99)00245-1.

25.   Aniceto, J. P. S.; Portugal, I.; Silva, C. M., Biomass-based polyols through oxypropylation reaction. *ChemSusChem* **2012,** *5* (8), 1358-1368, DOI 10.1002/cssc.201200032.

26.   Scarica, C.; Suriano, R.; Levi, M.; Turri, S.; Griffini, G., Lignin Functionalized with Succinic Anhydride as Building Block for Biobased Thermosetting Polyester Coatings. *ACS Sustainable Chem. Eng.* **2018,** *6* (3), 3392-3401, DOI 10.1021/acssuschemeng.7b03583.

27.   That, T., Cardanol-lignin-based polyurethanes. *Polym. Int.* **1996,** *41* (1), 13-16, DOI 10.1002/(SICI)1097-0126(199609)41:1<13::AID-PI557>3.0.CO;2-8.

28.   Griffini, G.; Passoni, V.; Suriano, R.; Levi, M.; Turri, S., Polyurethane coatings based on chemically unmodified fractionated lignin. *ACS Sustainable Chem. Eng.* **2015,** *3* (6), 1145-1154, DOI 10.1021/acssuschemeng.5b00073.

29.   Calvo-Correas, T.; Santamaria-Echart, A.; Saralegi, A.; Martin, L.; Valea, Á.; Corcuera, M. A.; Eceiza, A., Thermally-responsive biopolyurethanes from a biobased diisocyanate. *Eur. Polym. J.* **2015,** *70*, 173-185, DOI 10.1016/j.eurpolymj.2015.07.022.

30.   Sahoo, S.; Kalita, H.; Mohanty, S.; Nayak, S. K., Synthesis and characterization of vegetable oil based polyurethane derived from low viscous bio aliphatic isocyanate: Adhesion strength to wood-wood substrate bonding. *Macromol. Res.* **2017,** *25* (8), 772-778, DOI 10.1007/s13233-017-5080-2.

31.   Fache, M.; Viola, A.; Auvergne, R.; Boutevin, B.; Caillol, S., Biobased epoxy thermosets from vanillin-derived oligomers. *Eur. Polym. J.* **2015,** *68*, 526-535, DOI 10.1016/j.eurpolymj.2015.03.048.

32.   Wang, P.; Liu, S.; Deng, Y., Important Green Chemistry and Catalysis: Non-phosgene Syntheses of Isocyanates – Thermal Cracking Way. *Chin. J. Chem.* **2017,** *35* (6), 821-835, DOI 10.1002/cjoc.201600745.

33.   Hojabri, L.; Kong, X.; Narine, S. S., Fatty Acid-Derived Diisocyanate and Biobased Polyurethane Produced from Vegetable Oil: Synthesis, Polymerization, and Characterization. *Biomacromolecules* **2009,** *10* (4), 884-891, DOI 10.1021/bm801411w.

34.   Chung, J. W.; Park, J. H.; Choi, H. M.; Oh, K. W., Synthesis and characterization of a dyeable bio-based polyurethane/branched poly(ethylene imine) interpenetrating polymer network with enhanced wet fastness. *Text. Res. J.* **2019,** *89* (3), 335-346, DOI 10.1177/0040517517743739.

35.   Schemmer, B.; Kronenbitter, C.; Mecking, S., Thermoplastic Polyurethane Elastomers with Aliphatic Hard Segments Based on Plant-Oil-Derived Long-Chain Diisocyanates. *Macromol. Mater. Eng.* **2018,** *303* (4), 1700416, DOI doi:10.1002/mame.201700416.

36.   Tan, A. C. W.; Polo-Cambronell, B. J.; Provaggi, E.; Ardila-Suárez, C.; Ramirez-Caballero, G. E.; Baldovino-Medrano, V. G.; Kalaskar, D. M., Design and development of low cost polyurethane

biopolymer based on castor oil and glycerol for biomedical applications. *Biopolymers* **2018,** *109* (2), DOI 10.1002/bip.23078.

37.   Parcheta, P.; Datta, J., Environmental impact and industrial development of biorenewable resources for polyurethanes. *Crit. Rev. Environ. Sci. Technol.* **2017,** *47* (20), 1986-2016, DOI 10.1080/10643389.2017.1400861.

38.   Passoni, V.; Scarica, C.; Levi, M.; Turri, S.; Griffini, G., Fractionation of Industrial Softwood Kraft Lignin: Solvent Selection as a Tool for Tailored Material Properties. *ACS Sustainable Chem. Eng.* **2016,** *4* (4), 2232-2242, DOI 10.1021/acssuschemeng.5b01722.

39.   Allegretti, C.; Fontanay, S.; Krauke, Y.; Luebbert, M.; Strini, A.; Troquet, J.; Turri, S.; Griffini, G.; D'Arrigo, P., Fractionation of Soda Pulp Lignin in Aqueous Solvent through Membrane-Assisted Ultrafiltration. *ACS Sustainable Chem. Eng.* **2018,** *6* (7), 9056-9064, DOI 10.1021/acssuschemeng.8b01410.

40.   Allegretti, C.; Fontanay, S.; Rischka, K.; Strini, A.; Troquet, J.; Turri, S.; Griffini, G.; D'Arrigo, P., Two-step fractionation of a model technical lignin by combined organic solvent extraction and membrane ultrafiltration. *ACS Omega* **2019,** *4* (3), 4615-4626, DOI 10.1021/acsomega.8b02851.

41.   Balakshin, M.; Capanema, E., On the quantification of lignin hydroxyl groups with 31P and 13C NMR spectroscopy. *J. Wood Chem. Technol.* **2015,** *35* (3), 220-237, DOI 10.1080/02773813.2014.928328.

42.   Kuhire, S. S.; Nagane, S. S.; Wadgaonkar, P. P., Poly(ether urethane)s from aromatic diisocyanates based on lignin-derived phenolic acids. *Polym. Int.* **2017,** *66* (6), 892-899, DOI 10.1002/pi.5333.

43.   Bräse, S.; Gil, C.; Knepper, K.; Zimmermann, V., Organic azides: An exploding diversity of a unique class of compounds. *Angew. Chem. Int. Ed.* **2005,** *44* (33), 5188-5240, DOI 10.1002/anie.200400657.

44.   Constant, S.; Wienk, H. L. J.; Frissen, A. E.; Peinder, P. D.; Boelens, R.; Van Es, D. S.; Grisel, R. J. H.; Weckhuysen, B. M.; Huijgen, W. J. J.; Gosselink, R. J. A.; Bruijnincx, P. C. A., New insights into the structure and composition of technical lignins: A comparative characterisation study. *Green Chem.* **2016,** *18* (9), 2651-2665, DOI 10.1039/c5gc03043a.

45.   Son, D.; Gu, S.; Choi, J. W.; Suh, D. J.; Jae, J.; Choi, J.; Ha, J. M., Production of phenolic hydrocarbons from organosolv lignin and lignocellulose feedstocks of hardwood, softwood, grass and agricultural waste. *J. Ind. Eng. Chem.* **2019,** *69*, 304-314, DOI 10.1016/j.jiec.2018.09.009.

46.   Ma, Z.; Li, S.; Fang, G.; Patil, N.; Yan, N., Modification of chemical reactivity of enzymatic hydrolysis lignin by ultrasound treatment in dilute alkaline solutions. *Int. J. Biol. Macromol.* **2016,** *93*, 1279-1284, DOI 10.1016/j.ijbiomac.2016.09.095.

47.   Ding, Z.; Qiu, X.; Fang, Z.; Yang, D., Effect of Molecular Weight on the Reactivity and Dispersibility of Sulfomethylated Alkali Lignin Modified by Horseradish Peroxidase. *ACS Sustainable Chem. Eng.* **2018,** *6* (11), 14197-14202, DOI 10.1021/acssuschemeng.8b02826.

48.   Shimizu, S.; Yokoyama, T.; Akiyama, T.; Matsumoto, Y., Reactivity of lignin with different composition of aromatic syringyl/guaiacyl structures and Erythro/Threo side chain structures in β-O-4 type during alkaline delignification: As a basis for the different degradability of hardwood and softwood lignin. *J. Agric. Food Chem.* **2012,** *60* (26), 6471-6476, DOI 10.1021/jf301329v.

49.   Lourenço, A.; Gominho, J.; Marques, A. V.; Pereira, H., Reactivity of syringyl and guaiacyl lignin units and delignification kinetics in the kraft pulping of Eucalyptus globulus wood using Py-GC-MS/FID. *Bioresour. Technol.* **2012,** *123*, 296-302, DOI 10.1016/j.biortech.2012.07.092.

50.   Bondarenko, S. P.; Tiger, R. P.; Bagatur'yants, A. A.; Borisov, E. V.; Lebedev, V. L.; Éntelis, S. G., Quantum-chemical treatment of the mechanism of urethane formation by the extended Hückel method. *Russ Chem Bull* **1977,** *26* (2), 256-262, DOI 10.1007/BF00921826.

51.   Kim, S. H.; Choi, J.; Sakong, C.; Namgoong, J. W.; Lee, W.; Kim, D. H.; Kim, B.; Ko, M. J.; Kim, J. P., The effect of the number, position, and shape of methoxy groups in triphenylamine donors

on the performance of dye-sensitized solar cells. *Dyes Pigm.* **2015,** *113*, 390-401, DOI 10.1016/j.dyepig.2014.09.014.

52.   Klein, S. E.; Rumpf, J.; Kusch, P.; Albach, R.; Rehahn, M.; Witzleben, S.; Schulze, M., Unmodified kraft lignin isolated at room temperature from aqueous solution for preparation of highly flexible transparent polyurethane coatings. *RSC Adv.* **2018,** *8* (71), 40765-40777, DOI 10.1039/C8RA08579J.

53.   Avelino, F.; Miranda, I. P.; Moreira, T. D.; Becker, H.; Romero, F. B.; Taniguchi, C. A. K.; Mazzetto, S. E.; de Sá Moreira de Souza Filho, M., The influence of the structural features of lignin-based polyurethane coatings on ammonium sulfate release: kinetics and thermodynamics of the process. *J. Coat. Tech. Res.* **2018**, DOI 10.1007/s11998-018-0123-y.

54.   Bandekar, J.; Klima, S., FT-IR spectroscopic studies of polyurethanes Part I. Bonding between urethane COC groups and the NH Groups. *J. Mol. Struct.* **1991,** *263* (C), 45-57, DOI 10.1016/0022-2860(91)80054-8.

55.   Ciobanu, C.; Ungureanu, M.; Ignat, L.; Ungureanu, D.; Popa, V. I., Properties of lignin-polyurethane films prepared by casting method. *Ind. Crops Prod.* **2004,** *20* (2), 231-241, DOI 10.1016/j.indcrop.2004.04.024.

56.   Hussin, M. H.; Rahim, A. A.; Mohamad Ibrahim, M. N.; Brosse, N., Physicochemical characterization of alkaline and ethanol organosolv lignins from oil palm (Elaeis guineensis) fronds as phenol substitutes for green material applications. *Ind. Crops Prod.* **2013,** *49*, 23-32, DOI 10.1016/j.indcrop.2013.04.030.

57.   Shrestha, B.; Le Brech, Y.; Ghislain, T.; Leclerc, S.; Carré, V.; Aubriet, F.; Hoppe, S.; Marchal, P.; Pontvianne, S.; Brosse, N.; Dufour, A., A Multitechnique Characterization of Lignin Softening and Pyrolysis. *ACS Sustainable Chem. Eng.* **2017,** *5* (8), 6940-6949, DOI 10.1021/acssuschemeng.7b01130.

58.   Xinya, L.; Weiss, R. A., Relationship between the Glass Transition Temperature and the Interaction Parameter of Miscible Binary Polymer Blends. *Macromolecules* **1992,** *25* (12), 3242-3246, DOI 10.1021/ma00038a033.

59.   Mishra, A. K.; Narayan, R.; Raju, K. V. S. N.; Aminabhavi, T. M., Hyperbranched polyurethane (HBPU)-urea and HBPU-imide coatings: Effect of chain extender and NCO/OH ratio on their properties. *Prog. Org. Coat.* **2012,** *74* (1), 134-141, DOI 10.1016/j.porgcoat.2011.11.027.

60.   Lee, J. C.; Kim, B. K., Basic structure–property behavior of polyurethane cationomers. *J. Polym. Sci. Part A* **1994,** *32* (10), 1983-1989, DOI 10.1002/pola.1994.080321022.

61.   Domínguez, J. C.; Oliet, M.; Alonso, M. V.; Gilarranz, M. A.; Rodríguez, F., Thermal stability and pyrolysis kinetics of organosolv lignins obtained from Eucalyptus globulus. *Ind. Crops Prod.* **2008,** *27* (2), 150-156, DOI 10.1016/j.indcrop.2007.07.006.

62.   Nadji, H.; Diouf, P. N.; Benaboura, A.; Bedard, Y.; Riedl, B.; Stevanovic, T., Comparative study of lignins isolated from Alfa grass (Stipa tenacissima L.). *Bioresour. Technol.* **2009,** *100* (14), 3585-3592, DOI 10.1016/j.biortech.2009.01.074.

63.   Zhu, S. W.; Shi, W. F., Flame retardant mechanism of hyperbranched polyurethane acrylates used for UV curable flame retardant coatings. *Polym. Degradation. Stab.* **2002,** *75* (3), 543-547, DOI 10.1016/S0141-3910(01)00257-9.

64.   de Haro, J. C.; Rodríguez, J. F.; Pérez, Á.; Carmona, M., Incorporation of azide groups into bio-polyols. *J. Clean. Prod.* **2016,** *138*, 77-82, DOI 10.1016/j.jclepro.2016.05.012.

65.   Bose, S. K.; Omori, S.; Kanungo, D.; Francis, R. C.; Shin, N. H., Mechanistic differences between kraft and soda/AQ pulping. Part 1: Results from wood chips and pulps. *J. Wood Chem. Technol.* **2009,** *29* (3), 214-226, DOI 10.1080/02773810902961104.

66.   Kanungo, D.; Francis, R. C.; Shin, N. H., Mechanistic differences between kraft and soda/AQ pulping. Part 2: Results from lignin model compounds. *J. Wood Chem. Technol.* **2009,** *29* (3), 227-240, DOI 10.1080/02773810902961112.

67.   Gao, S.; Zhao, J.; Wang, X.; Guo, Y.; Han, Y.; Zhou, J., Lignin structure and solvent effects on the selective removal of condensed units and enrichment of S-type lignin. *Polym.* **2018,** *10* (9), DOI 10.3390/polym10090967.

68.   Chan, C.-M., *Polymer surface modification and characterization*. GmbH & Co.: Germany, 1994.

69.   Homola, T.; Matoušek, J.; Kormunda, M.; Wu, L. Y. L.; Černák, M., Plasma treatment of glass surfaces using diffuse coplanar surface barrier discharge in ambient air. *Plasma Chem. Plasma Process.* **2013,** *33* (5), 881-894, DOI 10.1007/s11090-013-9467-3.

70.   Chauhan, M.; Gupta, M.; Singh, B.; Singh, A. K.; Gupta, V. K., Effect of functionalized lignin on the properties of lignin-isocyanate prepolymer blends and composites. *Eur. Polym. J.* **2014,** *52* (1), 32-43, DOI 10.1016/j.eurpolymj.2013.12.016.

71.   De Haro, J. C.; Magagnin, L.; Turri, S.; Griffini, G., Lignin-Based Anticorrosion Coatings for the Protection of Aluminum Surfaces. *ACS Sustainable Chem. Eng.* **2019,** *7* (6), 6213-6222, DOI 10.1021/acssuschemeng.8b06568.

72.   Turkenburg, D. H.; van Bracht, H.; Funke, B.; Schmider, M.; Janke, D.; Fischer, H. R., Polyurethane adhesives containing Diels–Alder-based thermoreversible bonds. *J. Appl. Polym. Sci.* **2017,** *134* (26), DOI 10.1002/app.44972.

73.   Caretto, A.; Passoni, V.; Brenna, N.; Sitta, M.; Ogliosi, L.; Catel, G.; Turri, S.; Griffini, G., Fully Biobased Polyesters Based on an Isosorbide Monomer for Coil Coating Applications. *ACS Sustainable Chem. Eng.* **2018,** *6* (11), 14125-14134, DOI 10.1021/acssuschemeng.8b02659.

For Table of Contents Only
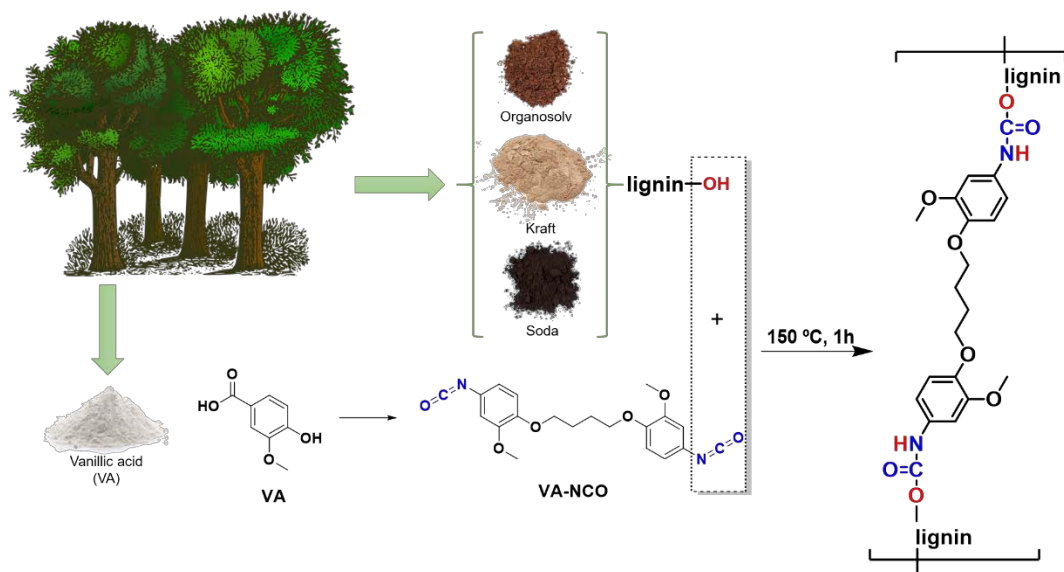
Synopsis

Lignin-based polyurethane coatings with high biomass content and tailored properties by lignin selection were successfully synthesized and characterized.